NEOPLASIA
www.neoplasia.com

Volume 33 Number xxx Month 2022 pp. 100836

Original Research

Analysis of RANK-c interaction partners identifies TRAF3 as a critical regulator of breast cancer aggressiveness

Chaido Sirinian[a,1,*]; Anastasios D. Papanastasiou[b,1]; Ozge Karayel[c]; Soren E. Degn[d]; Stavros Peroukidis[e]; Dimitrios Chaniotis[b]; Afrodite Nonni[f]; Maria Repanti[g]; Mark Kriegsmann[h]; Thomas Makatsoris[a]; Angelos Koutras[a]; Matthias Mann[c]; Haralabos P. Kalofonos[a]

[a] Molecular Oncology Laboratory, Division of Oncology, Department of Medicine, University of Patras, Patras, Greece
[b] Department of Biomedical Sciences, University of West Attica, Athens, Greece
[c] Department of Proteomics and Signal Transduction, Max-Planck Institute of Biochemistry, Planegg, Germany
[d] Department of Biomedicine, Aarhus University, Aarhus C, Denmark
[e] Panarkadikon General Hospital, Tripolis, Greece
[f] 1st Dept of Pathology, School of Medicine, National and Kapodistrian University of Athens, Athens, Greece
[g] Department of Pathology, Patras General Hospital, Patras, Greece
[h] Institute of Pathology, University of Heidelberg, Heidelberg, Germany

Abstract

Breast cancer is a highly heterogeneous disease both at the histological and molecular levels. We have previously shown that RANK-c is a regulator of NF-κB signaling and exerts a suppressive effect on aggressive properties of ER negative breast cancer cells, while there is an opposite effect on ER positive cell lines. In order to identify molecular determinants that govern the opposing function of RANK-c in breast cancer cells we employed the two cell lines with the highest degree of phenotypic divergence upon RANK-c-expression (SKBR3 and BT474) and identified proteins that interact with RANK-c by affinity-enrichment mass spectrometry (AE-MS) analysis. Annotating enriched proteins with NF-κB signaling pathway revealed TRAF3 as an interacting partner of RANK-c in SKBR3 cell protein lysates, but not in BT474 breast cancer cells in which RANK-c induces cell aggressiveness. To determine the role of TRAF3 in the phenotype of BT474-RANK-c cells, we reconstructed the TRAF3/RANK-c interaction both in parental BT474 and RANK-c expressing cells and tested for aggressive properties through colony formation, migration and invasion assays. TRAF3 forced expression was able to reverse BT474 phenotypic changes imposed by RANK-c, rendering cells less aggressive. Finally, *TRAF3* gene expression data and TRAF3 immunohistochemical (IHC) analysis on breast cancer samples indicated that TRAF3 expression correlates with Overall Survival (OS), Recurrence Free Survival (RFS) and several clinicopathological parameters (histological grade, proliferation index) of breast cancer disease.

Neoplasia (2022) 33, 100836

Keywords: Breast cancer, NF-κB, RANK-c, TRAF3, Aggressiveness, AE-MS

Introduction

Breast cancer affects one in 8 women throughout their lifetime [1]. While breast cancer is a highly heterogeneous disease, with multiple molecular subtypes (Luminal A, Luminal B, etc.), in everyday clinical practice two molecular parameters bear a significant relevance to prognosis and treatment

* Corresponding author.
E-mail address: hsirinian@upatras.gr (C. Sirinian).
[1] These authors contributed equally.
Received 13 May 2022; accepted 25 August 2022

https://doi.org/10.1016/j.neo.2022.100836

outcomes: hormone receptor status (ER and PR) and HER2 protein expression [2]. Hormone receptor (HR) positive breast cancer seems to be a significantly different disease entity in comparison to HR-negative breast cancer concerning disease biology, progression and patient outcomes [3,4].

The NF-κB pathway has important roles both in health and disease [5,6]. NF-κB activation can be spatiotemporally divided in two major pathways: the classical and the alternative NF-κB activation pathway. These pathways can have additive, independent or opposing cellular effects and they employ a different set of protein homodimers or heterodimers as active transcription factor elements (p65, p52, p50, RelB, c-Rel) [7]. In breast cancer NF-κB pathway activity has been correlated with HER2-positive and triple negative (ER-, PR-, HER2-) disease, aggressive phenotypes and poor patient outcomes [8,9]. However, due to the complexity of the NF-κB pathway and the immense heterogeneity of breast cancer, the role of each pathway (classical and alternative) in breast cancer development, progression and metastasis remains to be elucidated [10].

Tumor necrosis factor (TNF) receptor-associated factors (TRAFs) are a family of intracellular proteins that function downstream of multiple receptor signaling pathways, with TNF receptors (TNFRSF1A and TNFRSF1B) being the prototypical model of TRAF interaction and function [11,12]. After receptor activation, TRAFs function as adapter molecules with E3 ubiquitin ligase activity that mediate a plethora of cytoplasmic signaling cascades, with central roles in the biology of immune cells but also cancer [13]. TRAF-related signaling is involved in the activation of several transcription factor pathways, such as nuclear factor-κB (NF-κB), mitogen-activated protein kinases (MAPKs), and interferon-regulatory factors (IRFs) [14]. Notably, a major biological role of TRAFs is their capacity to positively or negatively regulate canonical and alternative NF-κB signaling in a cell-context-dependent manner. Generally, TRAF2, 5, and 6 are activators or/and enhancers of the canonical NF-κB signaling pathway, while TRAF3 acts mainly as an inhibitor of the alternative NF-κB pathway, through Nuclear Factor-κB-Kinase (NIK) degradation [15].

RANK (Receptor Activator of NF-κB) receptor belongs to the TNF receptor superfamily and upon ligand binding activates both the classical and alternative pathways through TRAF interactions [16–18]. Recently we were able to identify and characterize an alternatively spliced isoform of the *TNFSRF11A* (*RANK*) gene, named RANK-c, with the capacity to alter NF-κB pathway activation in a cell-context dependent manner in breast cancer [19,20]. RANK-c acts mainly through its interaction with TRAFs and especially TRAF2, a major regulator of NF-κB signaling pathway with a role both in the classical and alternative pathway [20]. Here we explore the opposing functions of RANK-c in breast cancer cells, and we identify TRAF3 as an important regulator of breast cancer aggressiveness that correlate with multiple clinicopathological parameters both at the mRNA and protein levels.

Materials and methods

Cell cultures, plasmids and antibodies

Breast cancer cell lines SKBR3 and BT474 were purchased from ATCC and cultured in 37°C, 5%CO_2, in DMEM medium with 10%FBS and pen/strep. The SKBR3-RANK-c and BT474-RANK-c stable cell lines were generated by electroporation using Amaxa® cell line nucleofector® Kit C for SKBR3 and Kit V for BT474 (LONZA, Walkersville, MD, USA). For transient transfection jetPRIME® reagent was employed (Polyplus-transfection S.A, USA).

PCR amplified RANK-c cDNA was cloned into a pCDNA3.1/Hygro(-) vector (Invitrogen). pcDNA3 HA-hTRAF3 (1098) was a kind gift from Michael Karin (Addgene plasmid # 66927; http://n2t.net/addgene:66927; RRID: Addgene_66927) and pcDNA-HA-hTRAF3 1-448 was a kind gift from Shao-Cong Sun (Addgene plasmid # 44033; http://n2t.net/addgene:44033; RRID: Addgene_44033) [21].

The antibodies employed in this study were: Fibronectin (sc-52331; 1:200, SCBT), Snail (SN9H2, #4719; 1:1000, CST), RANK (af683; 1:400, R&D systems), actin (MAB1501; 1:1000, Millipore, MA), IκB-α (112B2, #9247; 1:1000, CST), p-IκB-α (sc-8404; 1:200, SCBT), p65 (D14E12, #8242; 1:1000, CST), phospho-NF-κB p65 (93H1, #3033; 1:1000, CST), NIK (sc-8417; 1:200, SCBT), NF-κB2 p100/p52 (18D10, #3017; 1:1000, CST), RELB (sc-226; 1:200, SCBT), TRAF3 (sc-6933; 1:200, SCBT) for WB, TRAF3 (NB100-56176; 1:800, Novus Biologicals) for IHC, TRAF2 (sc-136999; 1:200, SCBT) for precipitation, TRAF2 (sc-877; 1:200, SCBT) for immunoblotting, TRAF6 (D21G3, #8028; 1:1000, CST), HER2/ErbB2 (#2242; 1:1000, CST), EGFR (E235,04-338; 1:4000, Millipore, MA), phospho-p44/42 (ERK1/2) (20G11, #4376; 1:1000, CST), p52 (sc-298; 1:200, SCBT).

Sample preparation and mass spectrometry analysis

Cells were lysed in 0.5% NP-40 lysis buffer (150 mM NaCl, 20 mM HEPES, 0.5 mM EDTA, 1 mM Na_3VO_4, proteinase inhibitor cocktail (Calbiochem)). Cell extracts from each condition were incubated overnight with 6 μg of RANK (AF-683) antibody at 4°C and next day retrieved with 20 μl Dynabeads protein G (Invitrogen) for 2 h at 4°C. Immunoprecipitates were washed three times in lysis buffer to remove unbound proteins. Beads were washed three times with 20 mM Hepes buffer PH 7.5 and resuspended in 1% SDC buffer (1% sodium deoxycholate in 100 mM Tris pH 8.5). TCEP and 2-Chloroacetamide to the final volumes of 10 mM and 40 mM, respectively, and 500 ng trypsin were added to each sample. Samples were subsequently incubated overnight at 37°C with agitation (1500 rpm). Next day, peptides were loaded onto StageTips loaded with SDB-RPS disks in loading buffer (1% TFA in isopropanol) and desalted as described in Kulak et al, 2014 [22]. Briefly, the StageTips were centrifuged at 1000 *g* for washing with loading buffer and 2% ACN/0.2% TFA and at 500*g* for elution with 80% ACN/0.1% TFA. The eluate was evaporated to dryness using a vacuum centrifuge and peptides were resuspended in MS loading buffer (2% ACN/0.2% TFA. Equal amount of peptides was subjected to LC-MS/MS analysis.

Peptides were separated on a 50 cm reversed-phase column (75 μm inner diameter, packed in-house with ReproSil-Pur C18-AQ 1.9 μm resin [Dr. Maisch GmbH]) with a binary buffer system of buffer A (0.1% formic acid (FA)) and buffer B (80% acetonitrile plus 0.1% FA) over 60 min gradient (steps: (1) 5–30% of buffer B for 35 min, (2) 30%–65% for 5 min, (3) 65-95% for 5 min, (4) staying at 95% for 5 min, (5) 95%-5% for 5 min and (6) staying at 5% for 5 min) using the EASY-nano LC 1200 system (Thermo Fisher Scientific) with a flow rate of 300 nL/min. Column temperature was maintained at 60°C. The nano LC system was coupled to Orbitrap Exploris 480 mass spectrometer (Thermo Fisher Scientific). The instrument is operated in Top12 DDA mode. We acquired full scans (300–1650 m/z, maximum injection time 25 ms, resolution 60,000 at 200 m/z, charges included 2-5 and dynamic exclusion of 30 ms) at a target of 3e6 ions. The 12 most intense ions were isolated and fragmented with higher-energy collisional dissociation (HCD) (target 1e5 ions, maximum injection time 28 ms, isolation window 1.4 m/z, NCE 28%) and detected in the Orbitrap (resolution 15,000 at 200 m/z).

Migration and Invasion assay

For the Migration assay (Transwell chambers, Corning Inc. NY) and Invasion assay (Matrigel, Conring Inc.) on the day of the experiment, culture chambers were incubated with serum free medium for 2 h in 37°C/5% CO_2 incubator. 2 × 10^5 cells/chamber (migration) and 2 × 10^4cells/chamber (invasion) were resuspended in serum free medium and seeded in the upper chamber of the assay. For counting migrating and invading cells, the chamber's membrane was washed with 1xPBS, fixed 10 min with 4%PFA and

20 min with methanol and stained with Giemsa for 5 min. Non-migrating or non-invasive cells were removed with a cotton swab. Images were obtained using an inverted microscope (Axiovert 40 CFL, AxioCam ERc, Zeiss). Each experimental procedure was repeated at least three times.

Colony formation assay

Cells (2,5 × 10^4 cells/well) were suspended in 1 ml of 10% FBS DMEM containing 0.5% agarose and plated on a semisolid medium (DMEM with 10% FBS and 0.7% agarose) in a 12-well plate. Cells were then placed in a 37°C and 5% CO_2 incubator. The next day, 500 μl of 10%FBS DMEM was added in each well and changed every three days. Images were obtained using an inverted microscope (Axiovert 40 CFL, AxioCam ERc, Zeiss). All experiments were done in triplicates.

Data processing and bioinformatics analysis

Publicly available gene expression data for *TRAF3* in breast cancer patients was analyzed online through KMplotter (kmplot.com) [23] and GOBO (Gene expression-based Outcome for Breast cancer Online, co.bmc.lu.se/gobo/) [24].

Raw MS files were processed within the MaxQuant environment (version 1.6.1.13) with the MaxLFQ algorithm for label-free quantification and the integrated Andromeda search engine with FDR < 0.01 at the protein and peptide levels [25–27]. We included methionine (M) oxidation and acetylation (protein N-term) as variable and carbamidomethyl (C) as fixed modifications in the search. We allowed up to 2 missed cleavages for tryptic digestion and considered peptides with at least seven amino acids for identification. "Match between runs" was enabled with a matching time window of 0.7 min to allow the quantification of MS1 features which were not identified in each single measurement. Peptides and proteins were identified using a UniProt FASTA database from *Homo sapiens* (2015) containing 21,051 entries.

For MS data, the freely available software PERSEUS (version 1.6.1.3) was used to perform all statistical analyses [28]. First of all, the proteins identified only by site-modification or found in the decoy reverse database and the contaminants were filtered out and MaxLFQ intensities were taken for quantification after they were transformed into log2 scale. Three biological replicates of each pulldown were grouped and a minimum of three valid values was required in at least one group. Missing values were imputed based on a normal distribution (width = 0.3, down-shift = 1.8). Significance was assessed using two-sample student's t-test, which determines if the means of two groups are significantly different from each other, with a permutation-based FDR of 1% and 5% and an S0 value of 0.1.

Co-immunoprecipitation and immunoblotting

Cells were lysed in 0.5% NP-40 lysis buffer (150 mM NaCl, 20 mM HEPES, 0.5 mM EDTA, 1 mM Na_3VO_4, proteinase inhibitor cocktail (Calbiochem)). Cell extracts from each condition were incubated overnight with 6 μg of RANK (AF-683), 2 μg of TRAF2 (sc-136999), antibodies at 4°C and next day retrieved with 20 μl Dynabeads protein G (Invitrogen) for 2 h at 4°C. Immunoprecipitates were washed three times in lysis buffer to remove unbound proteins. Immunoprecipitates were resolved in 10% sodium dodecyl sulfatepolyacrylamide gel electrophoresis and transferred onto polyvinylidene difluoride membrane (Millipore) before immunoblotting with the appropriate antibodies overnight at 4°C. Primary antibody incubation was followed by incubation with a horseradish peroxidase-conjugated secondary antibody (anti-goat; AP180P, 1:3000, Millipore USA, anti-mouse; AP182P, 1:3000, Millipore USA and anti-rabbit; #7076, 1:3000, CST).

FFPE tissue samples

Breast carcinoma FFPE (Formalin Fixed Paraffin Embedded) samples were retrieved from the archives of the Department of Pathology, Patras General Hospital, Greece. The selected cases comprised invasive breast carcinoma of histological grade 1 (eleven patients), grade 2 (thirty-three patients) and grade 3 (twenty-four patients). Histopathological grading (Nottingham grading system) and immunohistochemistry evaluation of ER, PR, HER2, and Ki67 markers were done as part of the routine diagnostic procedure. This study was conducted according to the principles laid down by the Declaration of Helsinki. Ethical approval was granted through the bioethics committee of Patras University, Greece (approval protocol number 37436/16/12/2013). Clinicopathological parameters of the cohort are presented in detail in Supplementary table 2.

H/E staining, immunostaining and TRAF3 scoring

For immunofluorescence staining, cells were fixed in 4% paraformaldehyde (PFA) for 10 min and permeabilized with 0.3% Triton X-100 in PBS. Non-specific binding was blocked by incubating cells in blocking buffer with 3% (w/v) BSA and 10% (v/v) FBS in PBS. Fixed cells were incubated with primary antibodies as indicated. Cells were washed with 1xPBS containing 0.1% Tween 20 and incubated with the relevant secondary antibodies (Alexa Fluor, Molecular Probes, Invitrogen). After washing, nuclei were stained with Hoechst and mounted in mounting medium. Images were recorded on an Axioskop, Zeiss inverted microscope and Metasystems Isis software was used to process the images.

For Immunohistochemistry (IHC) staining, the protocol has been previously described [29]. In brief, 4 μm-thick paraffin sections were mounted on Superfrost Plus microscope slides (BDH Laboratory Supplies, Menzel) and sections were deparaffinized in xylene and rehydrated in descending concentrations of ethanol. Antigen retrieval was performed by microwave pretreatment for 15 min in 0.01 mol/L citric acid, pH 6.0 and endogenous peroxidase activity was blocked by immersion in methanol containing 0.2% hydrogen peroxide for 15 min. Non-specific binding was inhibited by treating tissue sections with 1% bovine serum albumin (BSA) for 30 min. Tissue sections were incubated overnight at 4°C with the primary antibody followed by the Dako REALTM EnVisionTM Detection System (Dako) for 30min. Immunoreactions were visualized by the application of 3,3'-diaminobenzidine (DAB). All slides were counterstained with hematoxylin, dehydrated in ascending ethanol concentrations, immersed in xylene, and mounted. Slides were scored for TRAF3 expression blindly by two expert pathologists. For each section an assessment was made for staining intensity in a common scale from 1 to 4. Grading of TRAF3 staining in cancer cells, was: 1 for absent or low expression, 2 for weak expression, 3 for moderate expression and 4 for strong staining. For statistical analysis, tumors having a final staining score of 1 and 2 were binned to a low expression group and were compared to tumors with scores of 3 and 4, as the high expression group.

Staining of breast cancer cell lines, to assess morphological changes, was performed by fixation with 4% PFA for 10min and staining with hematoxylin for 4 min.

Statistical analysis

Student's t test or Mann–Whitney *U* test was used for comparisons between groups. One-way analysis of variance was used for multiple group comparisons. Differences of categorical variables between groups were determined using Fisher's exact test. All experimental data (other than MS data) were analyzed with the SPSS program (SPSS® release 23.0, Chicago, IL, USA) and presented as the mean ± standard deviation. Any p value <0.05 was considered statistically significant (ns: $p \geq 0.05$, $^{*}p < 0.05$; $^{**}p < 0.01$, $^{***}p < 0.001$).

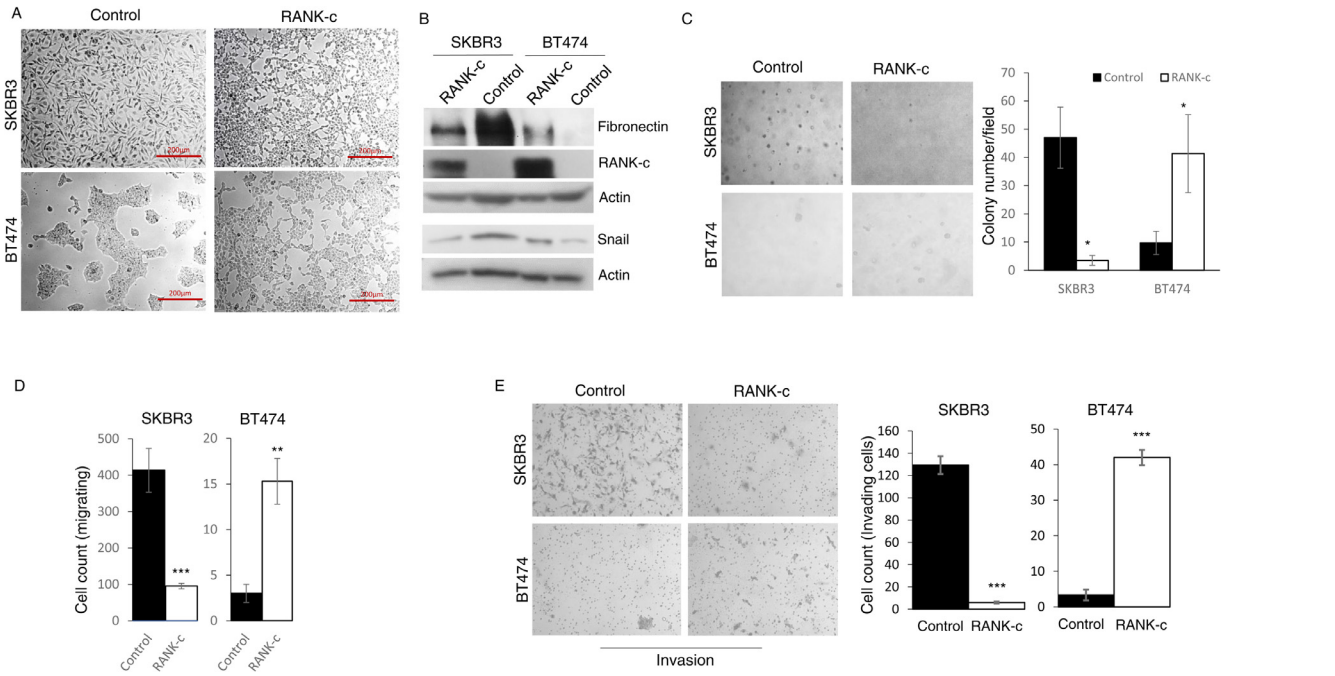

Fig. 1. RANK-c expression in SKBR3 and BT474 cells differentially affects aggressive properties. (A) Phase-contrast images of 2D cell cultures in standard media depicting morphological changes upon RANK-c expression. SKBR3-RANK-c cells lose their fibroblast-like appearance, while in the contrary BT474 cells lose coherence and attain a spindle-cell morphology. (B) Western blot of SKBR3 and BT474 cells extracts showing the downregulation and upregulation of Fibronectin and Snail upon RANK-c expression, respectively. (C) Representative images and quantification of colony formation by SKBR3-RANK-c and BT474-RANK-c cells in relevance to the respective control cells ($n = 3$ wells per group). (D) Transwell migration quantification for SKBR3-RANK-c, BT474-RANK-c and control cells ($n == 3$). (E) Matrigel invasion assay and quantification for SKBR3-RANK-c, BT474-RANK-c and control cells ($n == 3$).

Results

RANK-c induces opposite phenotypical effects in SKBR3 and BT474 breast cancer cells

We have previously shown that RANK-c exerts a suppressive effect on aggressive properties of ER-negative cells (MDA-MB-231, SKBR3), while ER-positive cells (BT474, MCF7) exhibit enhanced aggressiveness or remain unaffected by RANK-c expression [20]. In order to identify molecular determinants that regulate the opposing function of RANK-c in ER-negative and ER-positive breast cancer cells we employed the two cell lines (SKBR3 and BT474) that present the highest degree of phenotypic reversal upon RANK-c expression. For that, SKBR3-RANK-c cells that lose their aggressive properties and BT474-RANK-c cells that become more aggressive in comparison to control cells, were employed. While SKBR3-RANK-c cells, in 2D standard culturing conditions lost their characteristic cell morphology and aggressive properties, as also previously shown [20], BT474-RANK-c cells attained a discohesive appearance with spindle cell shape, in comparison with control cells, resembling a possible EMT ongoing process (Fig. 1A and Supplementary Fig. 1A). The possible EMT activation in BT474-RANK-c expressing cells was further corroborated by the characteristic upregulation of EMT-related proteins, Fibronectin and Snail (Fig. 1B). In addition, BT474-RANK-c cells enhanced their aggressive properties as indicated by a significant increase in their colony forming capacity in soft agar, in addition to an increase in their migration (transwell) and invasion capacity compared to control cells (Fig. 1C-E and Supplementary Fig. 1B). On the other hand, SKBR3-RANK-c cells presented with an opposite phenotype concerning migration, invasion and colony formation, in accordance with the already described role of RANK-c in ER-negative breast cancer cell lines [20]. The above data confirm that RANK-c expression differentially affects the two breast cancer cell lines in terms of cell morphology and functional traits relevant to cancer aggressiveness.

The NF-kB pathway is differentially regulated by RANK-c in SKBR3 and BT474 breast cancer cells

We have previously shown that forced expression of RANK-c in ER-negative breast cancer cell lines is able to inhibit stimuli-dependent activation of NF-κB and EGFR, in most part, by an intracellular RANK-c/TRAF2 and RANK-c/EGFR protein interaction [20]. Aiming to extend and further elaborate our findings in ER-positive cells we performed analyses of SKBR3 and BT474 cell extracts at standard culturing condition for HER2, EGFR, TRAFs and major NF-κB pathway proteins (Fig. 2A). Interestingly, western blot protein expression indicated that SKBR3-RANK-c cells present a diminished NF-κB activity while BT474-RANK-c had the opposite phenotype. More specifically, in SKBR3 cells that express RANK-c there is a shift from the classical to the alternative NF-κB pathway, shown by the concomitant phospho-p65 down regulation, IκB-alpha and NIK upregulation in western blots (Fig. 2A). However, the observed classical pathway downregulation (p-p65 downregulation, IκB-alpha upregulation) in parallel with the alternative pathway activation (NIK upregulation) leads to the loss of the classical pathway-dependent factors RELB and NFKB2 (p100 and p52) as also shown in Fig. 2A, leading to an overall disruption of NF-κB signaling in SKBR3 cells. Conversely, in BT474-RANK-c cells there is an upregulation of p65 phosphorylation with a concomitant decrease in IkB-alpha protein indicating an upregulation of the classical NF-κB pathway and a slight increase in the alternative pathway as judged by RELB and p100 induction (Fig. 2A). At the same time, BT474-RANK-c cells indicated a TRAF2 and HER2 protein upregulation, indicative of an excessive NF-κB and HER2-relevant pathway activation (Fig. 2A). Classical

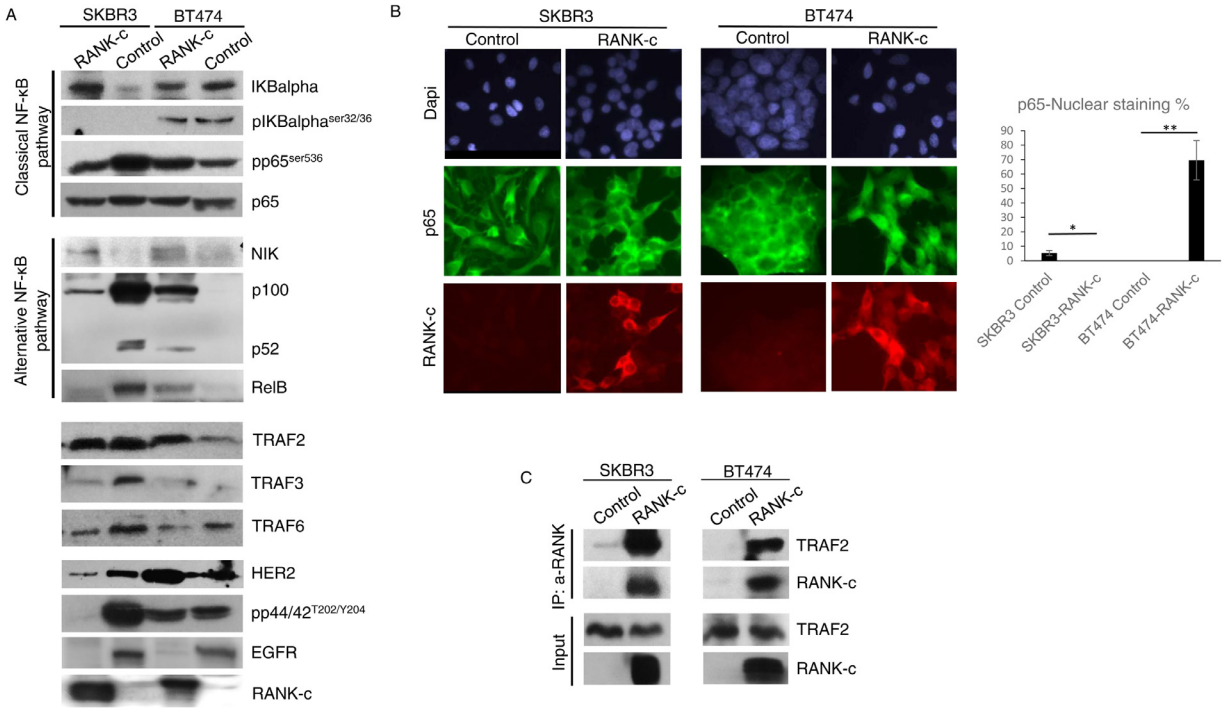

Fig. 2. RANK-c differentially affects multiple signalling pathways in SKBR3 and BT474 cells. (A) Western blot analyses for the indicated proteins in SKBR3 and BT474 cells (RANK-c and control). (B) Representative images and quantification of immunofluorescence staining of SKBR3-RANK-c, BT474-RANK-c and control cells for RANK-c and p65 protein localization. Split channels at 40x magnification. (C) Western blot analysis of RANK-c expressing SKBR3 and BT474 cell lysates immunoprecipitated with an antibody against RANK (AF683) and blotted for endogenous TRAF2 protein.

NF-κB pathway activation was further confirmed in BT474 cells through immunofluorescence imaging and quantification of the nuclear localization of p65 and p52 in RANK-c expressing cells (Fig. 2B and Supplementary Fig. 1C, D).

In order to pinpoint alterations in RANK-c protein function that could account for the differences in the NF-κB pathway between the two breast cancer cell lines, we focused on RANK-c interacting partners. TRAF2 is a major regulator of the NF-κB signaling pathway, and SKBR3- and BT474-RANK-c expressing cells were tested through co-immunoprecipitation assays for the NF-κB-relevant RANK-c/TRAF2 interaction. In both cell lines, RANK-c protein interacts with TRAF2 to a similar extent, indicating that the RANK-c/TRAF2 interaction is not responsible for the opposing cellular phenotypes and NF-κB activity observed in the cell lines studied (Fig. 2C). Collectively, these data identify NF-κB signaling upregulation as an important factor of breast cancer cell aggressiveness and at the same time point to another uncharacterized factor differentially affecting RANK-c/TRAF2 interaction outcome regarding functional cell properties.

TRAF3 differentially associates with the RANK-c/TRAF2 complex in SKBR3 and BT474 cells

To pinpoint the possible molecular alterations differentially affecting NF-κB activation and cell behavior in the two cell lines, we immunoprecipitated RANK-c from SKBR3 and BT474 cells and subjected those affinity-enriched samples to liquid-chromatography –tandem mass spectrometry (LC-MS/MS) analysis (AE-MS). As expected, TRAF2 was significantly enriched in RANK-c (TNFRSF11A)-enriched samples compared to the controls in both cell lines, confirming the previously characterized RANK-c/TRAF2 interaction. Furthermore, we annotated the AE-MS data for known protein complexes relevant to TRAF2 and NF-κB regulation and compared the RANK-c- enriched proteins in the two cell lines (Supplementary Table 1) [30,31]. Notably, TRAF3 was significantly enriched only in SKBR3-RANK-c cells (FDR<1%), suggesting a possible protein complex of RANK-c/TRAF2/TRAF3/BIRC2 reminiscent of the initial steps in alternative NF-κB activation (Fig. 3A). In contrast, in BT474-RANK-c cells, the only NF-κB-relevant TRAF2 interactors identified, except RANK-c, were BIRC2 and DIABLO, indicating that RANK-c through the TRAF2/BIRC2 interaction could initiate and sustain the classical NF-κB pathway (Fig. 3A) [32,33]. TRAF3 is a major regulator of the NF-κB pathway missing from the RANK-c protein complex of BT474 cells (Supplementary Fig. 1E) [34]. These findings were further confirmed through RANK-c immunoprecipitation and TRAF3 immunoblotting in SKBR3 and BT474 cells (Fig. 3B) and the interaction was also tested in 293T cells after transient transfection with the respective plasmid constructs (RANK-c, TRAF2, TRAF3) (Fig. 3C). The above data indicate that TRAF3 is a missing factor from the NF-κB-related complex TRAF2/RANK-c in BT474 cells, that might affect signaling outcome and cellular phenotype.

Forced expression of TRAF3 reverts aggressiveness of BT474-RANK-c cells

The BT474 breast cancer cell line seems to lack *TRAF3* expression both at the mRNA (Cancer Cell Encyclopedia, Broad 2019) and protein levels (Figs. S2A and 3B). In order to test the role of TRAF3 in BT474 cells, we transiently transfected both control and RANK-c expressing cells with a human TRAF3-expression plasmid construct and functionally characterized the effect of TRAF3 expression. Forced expression of TRAF3 significantly reduced soft agar colony forming capacity of BT474-RANK-c expressing cells but not control RANK-c expressing cells transfected with the empty plasmid vector (Fig. 4A). At the same time, forced expression of TRAF3 was able to revert the migratory and invasive phenotypes described for BT474-RANK-c cells to levels almost that of control cells (Fig. 4B and C). To further test

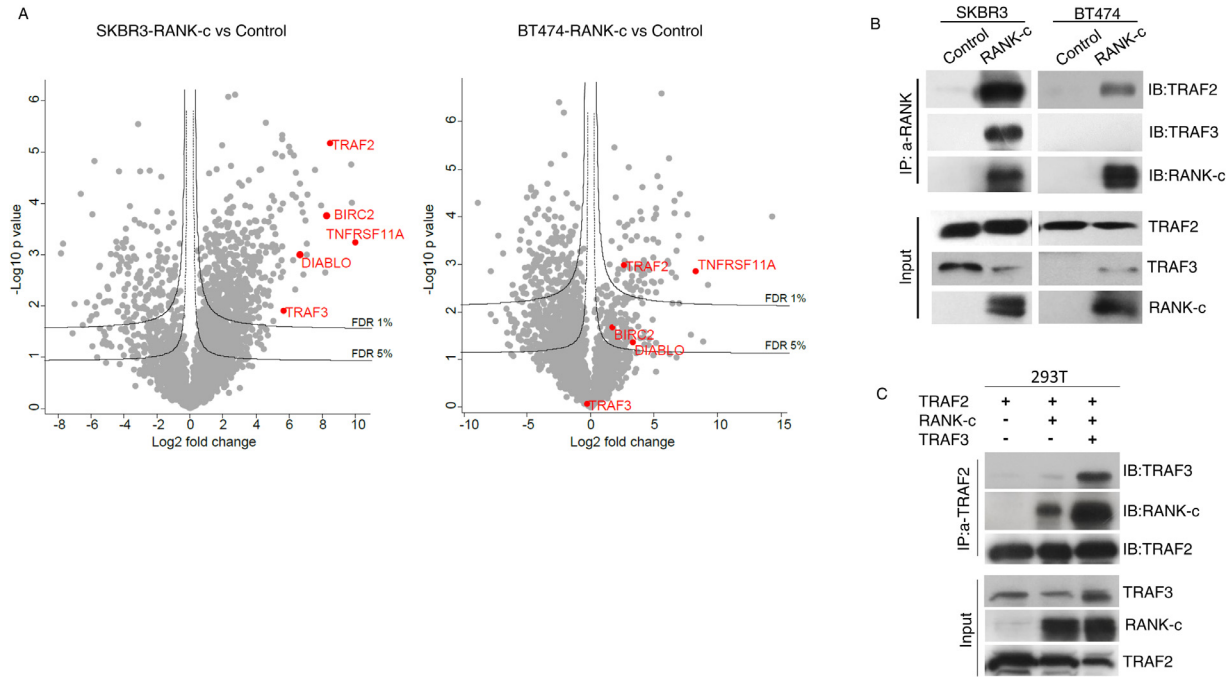

Fig. 3. TRAF3 is absent from the RANK-c/TRAF2 complex in BT474 cells. (A) Volcano plots of RANK-c-enriched samples compared to their controls in SKBR3 and BT474 cells. The lines represent significance cut-offs of a 1% and 5% FDR with an S0 value of 0.1. All proteins identified in this experiment are listed in Supplementary Table 1. (B) Western blot analysis of SKBR3-RANK-c and BT474-RANK-c cell lysates immunoprecipitated with an antibody against RANK (AF683) and blotted for endogenous TRAF2 and TRAF3 proteins. (C) Western blot analysis of 293T cells transiently transfected with the indicated plasmid constructs and subsequently lysed and immunoprecipitated with an antibody against TRAF2 (sc-136999) and blotted for RANK-c and TRAF3 proteins.

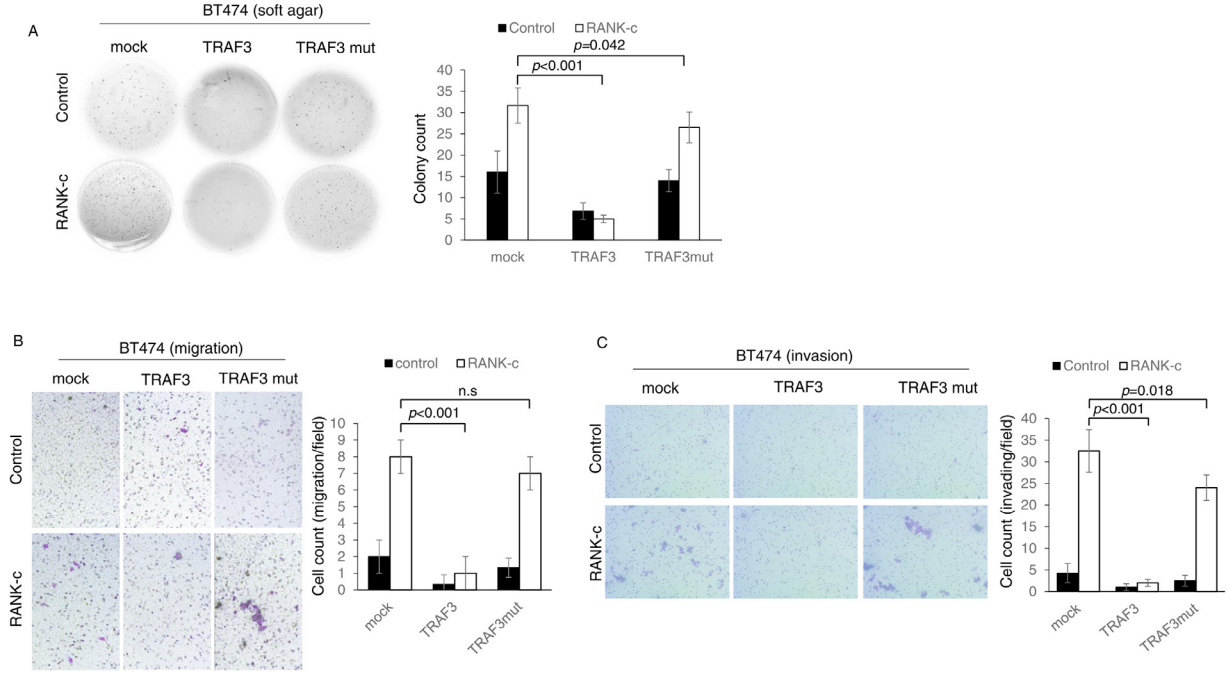

Fig. 4. Forced expression of TRAF3 in BT474-RANK-c cell is able to reverse the aggressive cell phenotype. (A) Colony formation assay and quantification of BT474-RANK-c and parental cells (control) transiently transfected with a TRAF3 plasmid or an inactive TRAF3 mutant plasmid (TRAF3mut). (B) Transwell migration assay and quantification of BT474-RANK-c and control cells after transient transfection with the indicated plasmid constructs for TRAF3 (TRAF3 and TRAF3mut). (C) Matrigel invasion assay and quantification of BT474-RANK-c and control cells after transient transfection with the indicated plasmid constructs (as for migration).

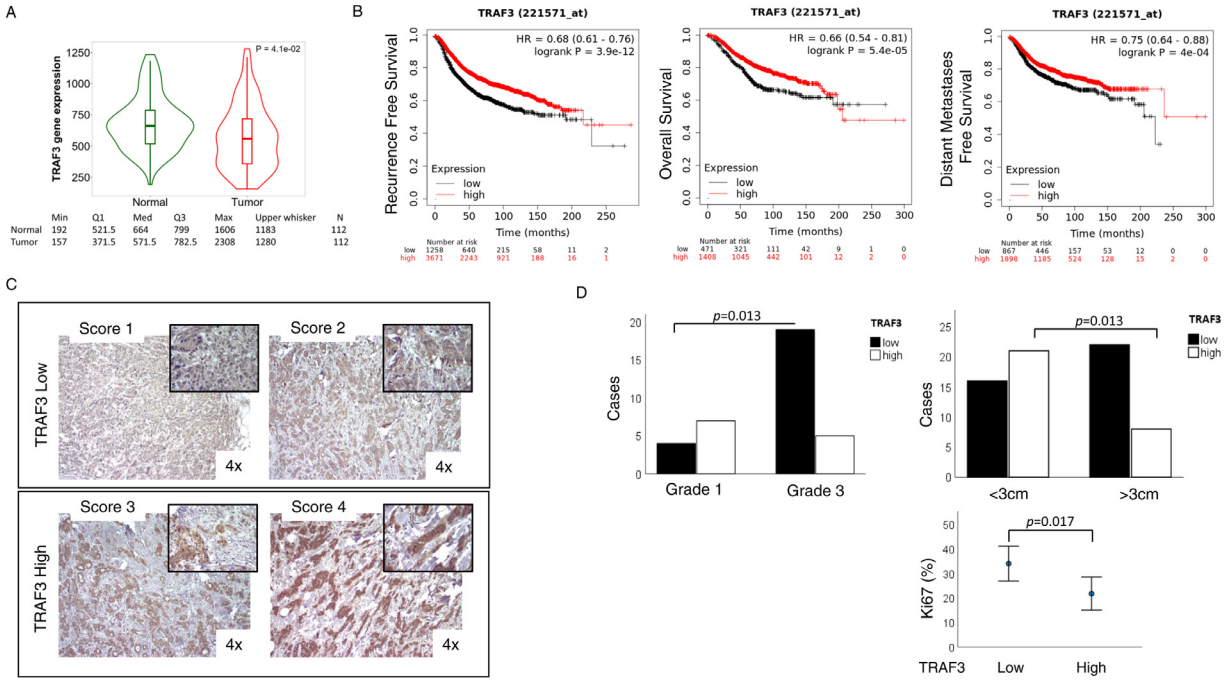

Fig. 5. TRAF3 expression is positively correlated with favourable prognosis in breast cancer patients. (A) mRNA expression of *TRAF3* in between normal mammary tissue and breast cancer (Kmplot.com). (B) Kaplan Mayer plots for RFS, OS and DFMS in an unselected cohort of breast cancer patients stratified based on *TRAF3* expression (Kmplot.com). (C) Representative images of immunohistochemical staining for TRAF3 protein in breast cancer FFPE samples depicting intensity levels and the scoring system employed in this study. Inserts are 10x magnifications of each representative image. (D) Correlation of TRAF3 expression in breast cancer FFPE samples with clinicopathological parameters in the cohort under study. High TRAF3 expression presents a statistically significant correlation with low grade tumours (G1), smaller tumour dimensions (>3cm) and lower proliferation index (ki67).

the specific role of TRAF3 absence in the aggressive phenotype of BT474-RANK-c expressing cells, we repeated the functional experiments employing a mutant TRAF3 plasmid construct (Fig. S2B) that is unable to bind NIK protein kinase. We found that a non-functional TRAF3 is unable to restore the BT474 wild-type phenotype in RANK-c expressing cells (Fig. 4A-C). These data identify TRAF3 as an important regulator of aggressive properties of BT474 breast cancer cells.

TRAF3 mRNA and protein levels correlate with breast cancer patient RFS, OS and clinicopathological parameters

In order to evaluate the potential role of TRAF3 in breast cancer patient's clinical outcome, we leveraged publicly available gene expression datasets for the *TRAF3* gene in breast cancer samples (KMplotter, kmplot.com/analysis). Gene expression levels of *TRAF3* were diminished in tumor samples compared to normal, indicating a possible inhibitory role of TRAF3 in the development of breast cancer (Fig. 5A). In addition, *TRAF3* expression was positively correlated with longer recurrence free survival (RFS), overall survival (OS) and distant metastases free survival (DMFS) in the whole breast cancer patient cohort employed in this analysis (Fig. 5B). To further support our findings, we employed GOBO (Gene expression-based Outcome for Breast cancer Online, co.bmc.lu.se/gobo/) and tested possible correlations of *TRAF3* gene expression with clinicopathological parameters. This analysis reconfirmed the positive correlation of *TRAF3* gene expression with longer OS and longer DMFS in the whole cohort, and intriguingly identified a positive correlation of *TRAF3* expression with negative LN status in the entire cohort ($p < 0.00001$) and a negative correlation with tumor size (SizeStrat) and tumor grade (GradeStrat) in multivariate analysis ($p < 0.00001$ and $p = 0.04$, respectively) (Fig. S2C).

To further elucidate the possible role of TRAF3 in breast cancer, we immunohistochemically (IHC) stained an unselected patient cohort of breast cancer FFPE samples ($n = 68$) (Supplementary table 2). TRAF3 scoring was made on a scale from 1 to 4 and then collapsed to TRAF3 Low (Score 1 and 2) cases and TRAF3 High (Score 3 and 4) cases in order to statistically correlate protein expression to available clinicopathological parameters (Fig. 5C). As a result, TRAF3 protein expression was found higher in low grade (Histological grade 1) cases and vice versa ($p = 0.013$), while TRAF3 presented an inverse correlation with tumor dimension and proliferation index ki67 in breast cancer patients ($p = 0.013$ and $p = 0.017$, respectively) (Fig. 5D). In total, our results identify TRAF3 as a negative regulator of breast cancer aggressiveness in unselected patient cohorts both at the mRNA and protein levels.

Discussion

Alternative splicing generates multiple gene transcripts and consequently relevant protein isoforms, expanding biological complexity and protein functionality [35]. Several splicing events in breast cancer modulate disease biology and progression [36,37]. We have previously identified RANK-c as an alternatively spliced transcript of the *TNFRSF11A* gene with a role in NF-κB regulation and breast cancer aggressiveness [20]. The NF-κB pathway is one of the most well studied intracellular signaling cascades, with important roles both in normal tissue but also in a plethora of malignancies [5,6]. Activated NF-κB transcription factor dimers have been identified in breast cancer cells and their nuclear expression is correlated with more aggressive disease [9]. RANK-c seems to be able to inhibit or induce NF-κB activity depending on cell type, and intriguingly, RANK-c presents an inhibitory effect when expressed in ER-negative breast cancer cells (MDA-MB-231, SKBR3), while it has the opposite effect in some ER-positive breast cancer cell lines (BT474), presenting a cell-type-specific pattern of action.

The function of a protein is often dependent on the interacting partners, which in many cases dictate functional outcomes [38]. With that in mind, we hypothesized that phenotypical differences produced through RANK-c expression in SKBR3 and BT474 cells could be attributed to different interacting partners. TRAF2, which was previously identified in complex with RANK-c in MDA-MB-231 cells was also identified in this work as an interactor of RANK-c in both SKBR3 and BT474 cells, thus excluding TRAF2 as the critical factor that differentiates cellular behavior. To approach our hypothesis in an unbiased, high-throughput way, we employed AE-MS analysis of RANK-c interactors from SKBR3-RANK-c and BT474-RANK-c cells. This analysis determined multiple possible interactors for RANK-c in each cell line, which we then curated for their relevance in the context of the NF-κB pathway. This analysis allowed us to identify TRAF3 protein to be absent from the RANK-c complex in BT474 cells, as also confirmed by co-immunoprecipitation and immunoblotting (Fig. S3). TRAF3 has a well-established role in NF-κB regulation in conjunction with other TRAF molecules, presenting an inhibitory function when it comes to NF-κB activation in B- cells [34,39]. However, little is known in relevance to TRAF3 function in breast cancer and whether it plays a significant role in tumor initiation, progression and metastasis [40,41].

To test TRAF3 action in breast cancer cells, we expressed TRAF3 and an inactive mutant form (TRAF3mut) in BT474 cells and analyzed aggressive properties through colony formation, migration and invasion assays. Forced expression of TRAF3 in control BT474 and RANK-c expressing cells attenuated cell motility and invasiveness as well as colony formation in a TRAF3 specific manner, indicating a possible inhibitory action of TRAF3 in breast cancer disease.

To further elucidate this possibility, we employed and analyzed publicly available gene expression data on breast cancer from KMplotter and GOBO relevant to *TRAF3* gene expression. This analysis showed that *TRAF3* expression positively correlates with better OS, RFS and DFMS of breast cancer patients, while *TRAF3* gene expression is reduced in breast cancer tissue in contrast to the normal mammary gland, supporting the notion that *TRAF3* could act as a tumor suppressor in breast tumorigenesis.

Finally, and because mRNA expression does not necessarily reflect protein expression and protein localization, we IHC stained an unselected cohort of breast cancer patients for TRAF3 protein. Our results indicated that TRAF3 has higher expression levels in Grade 1 (G1) cases in contrast to Grade 3 (G3), while at the same time protein levels present an inverse correlation with tumor dimensions and proliferation index (ki67). Our data on the role of TRAF3 in breast cancer, to our knowledge, for the first time suggest features of a tumor suppressor for this gene, and a favorable prognosis for breast cancer patients that express TRAF3. We suggest that future studies should explore the utility of this novel finding in a prognostic, predictive and potentially therapeutic context. Nevertheless, and while our preliminary data on the role of TRAF3 in breast cancer indicates features of a tumor suppressor and improved outcomes for patients that express TRAF3, the immense heterogeneity observed both at the molecular and histological levels in mammary malignant tumors, requires the engagement of a larger patient cohort and larger disease subgroups to fully validate these findings.

Declaration of Competing Interest

The authors declare that the research was conducted in the absence of any commercial or financial relationships that could be construed as a potential conflict of interest.

CRediT authorship contribution statement

Chaido Sirinian: Conceptualization, Methodology, Validation, Formal analysis, Investigation, Supervision. **Anastasios D. Papanastasiou:** Conceptualization, Methodology, Validation, Formal analysis, Investigation, Supervision, Data curation, Writing – original draft, Writing – review & editing. **Ozge Karayel:** Methodology, Validation, Formal analysis, Investigation, Writing – original draft. **Soren E. Degn:** Validation, Formal analysis, Writing – original draft, Writing – review & editing. **Stavros Peroukidis:** Data curation, Writing – original draft, Validation, Funding acquisition. **Dimitrios Chaniotis:** Formal analysis, Supervision, Writing – original draft. **Afrodite Nonni:** Formal analysis, Investigation, Writing – review & editing. **Maria Repanti:** Resources, Data curation, Writing – original draft. **Mark Kriegsmann:** Supervision, Writing – original draft, Writing – review & editing. **Thomas Makatsoris:** Supervision, Writing – original draft, Writing – review & editing. **Angelos Koutras:** Supervision, Writing – original draft, Writing – review & editing. **Matthias Mann:** Supervision, Writing – review & editing. **Haralabos P. Kalofonos:** Supervision, Funding acquisition, Writing – review & editing.

Acknowledgements

We are grateful to Michael Karin and Shao-Cong Sun for sharing TRAF3 plasmid constructs. This work was supported by partial funding from HeMoPe (Hellenic Society for Molecular Medicine and Personalized Diagnostics and Treatment; *hemope.org*). We thank Igor Paron and Duc Tung Vu for their technical assistants.

Supplementary materials

Supplementary material associated with this article can be found, in the online version, at doi:10.1016/j.neo.2022.100836.

References

[1] Tao Z, Shi A, Lu C, Song T, Zhang Z, Zhao J. Breast cancer: epidemiology and etiology. *Cell Biochem Biophys* 2015;**72**(2):333–8.

[2] Lopez-Garcia MA, Geyer FC, Lacroix-Triki M, Marchió C, Reis-Filho JS. Breast cancer precursors revisited: molecular features and progression pathways. *Histopathology* 2010;**57**(2):171–92.

[3] Weigelt B, Baehner FL, Reis-Filho JS. The contribution of gene expression profiling to breast cancer classification, prognostication and prediction: a retrospective of the last decade. *J Pathol* 2010;**220**(2):263–80.

[4] Reis-Filho JS, Pusztai L. Gene expression profiling in breast cancer: classification, prognostication, and prediction. *Lancet N Am Ed* 2011;**378**(9805):1812–23.

[5] Dolcet X, Llobet D, Pallares J, Matias-Guiu X. NF-kB in development and progression of human cancer. *Virchows Arch* 2005;**446**(5):475–82.

[6] Gilmore TD. NF-κB and human cancer: what have we learned over the past 35 years? *Biomedicines* 2021;**9**(8):889.

[7] Perkins ND. Integrating cell-signalling pathways with NF-κB and IKK function. *Nat Rev Mol Cell Biol* 2007;**8**(1):49–62.

[8] Perou CM, Sørlie T, Eisen MB, Van De Rijn M, Jeffrey SS, Rees CA, Pollack JR, Ross DT, Johnsen H, Akslen LA, Fluge Ø. Molecular portraits of human breast tumours. *Nature* 2000;**406**(6797):747–52.

[9] Biswas DK, Shi Q, Baily S, Strickland I, Ghosh S, Pardee AB, Iglehart JD. NF-κB activation in human breast cancer specimens and its role in cell proliferation and apoptosis. *Proc Natl Acad Sci* 2004;**101**(27):10137–42.

[10] Park YH. The nuclear factor-kappa B pathway and response to treatment in breast cancer. *Pharmacogenomics* 2017;**18**(18):1697–709.

[11] Ha H, Han D, Choi Y. TRAF-mediated TNFR-family signaling. *Curr Protoc Immunol* 2009;**87**(1):11–19.

[12] Lalani AI, Zhu S, Gokhale S, Jin J, Xie P. TRAF molecules in inflammation and inflammatory diseases. *Curr Pharmacol Rep* 2018;**4**(1):64–90.

[13] Xie P. TRAF molecules in cell signaling and in human diseases. *J Mol Signal* 2013;**8**(1):1–31.

[14] Inoue JI, Ishida T, Tsukamoto N, Kobayashi N, Naito A, Azuma S, Yamamoto T. Tumor necrosis factor receptor-associated factor (TRAF) family: adapter proteins that mediate cytokine signaling. *Exp Cell Res* 2000;**254**(1):14–24.

[15] Dhillon B, Aleithan F, Abdul-Sater Z, Abdul-Sater AA. The evolving role of TRAFs in mediating inflammatory responses. *Front Immunol* 2019;**10**:104.

[16] Galibert L, Tometsko ME, Anderson DM, Cosman D, Dougall WC. The involvement of multiple tumor necrosis factor receptor (TNFR)-associated factors in the signaling mechanisms of receptor activator of NF-κB, a member of the TNFR superfamily. *J Biol Chem* 1998;**273**(51):34120–7.

[17] Darnay BG, Haridas V, Ni J, Moore PA, Aggarwal BB. Characterization of the intracellular domain of receptor activator of NF-κB (RANK): interaction with tumor necrosis factor receptor-associated factors and activation of NF-κB and c-Jun N-terminal kinase. *J Biol Chem* 1998;**273**(32):20551–5.

[18] Wong BR, Josien R, Lee SY, Vologodskaia M, Steinman RM, Choi Y. The TRAF family of signal transducers mediates NF-κB activation by the TRANCE receptor. *J Biol Chem* 1998;**273**(43):28355–9.

[19] Papanastasiou AD, Sirinian C, Kalofonos HP. Identification ofel human receptor activator of nuclear factor-kB isoforms generated through alternative splicing: implications in breast cancer cell survival and migration. *Breast Cancer Res* 2012;**14**(4):1–6.

[20] Sirinian C, Papanastasiou AD, Schizas M, Spella M, Stathopoulos GT, Repanti M, Zarkadis IK, King TA, Kalofonos HP. RANK-c attenuates aggressive properties of ER-negative breast cancer by inhibiting NF-κB activation and EGFR signaling. *Oncogene* 2018;**37**(37):5101–14.

[21] Liao G, Zhang M, Harhaj EW, Sun SC. Regulation of the NF-κB-inducing kinase by tumor necrosis factor receptor-associated factor 3-induced degradation. *J Biol Chem* 2004;**279**(25):26243–50.

[22] Kulak NA, Pichler G, Paron I, Nagaraj N, Mann M. Minimal, encapsulated proteomic-sample processing applied to copy-number estimation in eukaryotic cells. *Nat Methods* 2014;**11**(3):319–24.

[23] Győrffy B. Survival analysis across the entire transcriptome identifies biomarkers with the highest prognostic power in breast cancer. *Comput Struct Biotechnol Jo* 2021;**19**:4101–9.

[24] Ringnér M, Fredlund E, Häkkinen J, Borg Å, Staaf J. GOBO: gene expression-based outcome for breast cancer online. *PLoS One* 2011;**6**(3):e17911.

[25] Cox J, Mann M. MaxQuant enables high peptide identification rates, individualized ppb-range mass accuracies and proteome-wide protein quantification. *Nat Biotechnol* 2008;**26**(12):1367–72.

[26] Cox J, Neuhauser N, Michalski A, Scheltema RA, Olsen JV, Mann M. Andromeda: a peptide search engine integrated into the MaxQuant environment. *J Proteome Res* 2011;**10**(4):1794–805.

[27] Cox J, Hein MY, Luber CA, Paron I, Nagaraj N, Mann M. Accurate proteome-wide label-free quantification by delayed normalization and maximal peptide ratio extraction, termed MaxLFQ. *Mol Cell Proteomics* 2014;**13**(9):2513–26.

[28] Tyanova S, Temu T, Sinitcyn P, Carlson A, Hein MY, Geiger T, Mann M, Cox J. The Perseus computational platform for comprehensive analysis of (prote) omics data. *Nat Methods* 2016;**13**(9):731–40.

[29] Sirinian C, Symeonidis A, Giannakoulas N, Zolota V, Melachrinou M. Overexpression of phosphorylated p27Kip1 at threonine 187 may predict outcome in aggressive B-cell lymphomas. *Leuk Lymphoma* 2011;**52**(5):814–22.

[30] Takeuchi M, Rothe M, Goeddel DV. Anatomy of TRAF2: distinct domains for nuclear factor-κB activation and association with tumor necrosis factor signaling proteins. *J Biol Chem* 1996;**271**(33):19935–42.

[31] Zarnegar BJ, Wang Y, Mahoney DJ, Dempsey PW, Cheung HH, He J, Shiba T, Yang X, Yeh WC, Mak TW, Korneluk RG. Noncanonical NF-κB activation requires coordinated assembly of a regulatory complex of the adaptors cIAP1, cIAP2, TRAF2 and TRAF3 and the kinase NIK. *Nat Immunol* 2008;**9**(12):1371–8.

[32] He L, Grammer AC, Wu X, Lipsky PE. TRAF3 forms heterotrimers with TRAF2 and modulates its ability to mediate NF-κB activation. *J Biol Chem* 2004;**279**(53):55855–65.

[33] Borghi A, Verstrepen L, Beyaert R. TRAF2 multitasking in TNF receptor-induced signaling to NF-κB, MAP kinases and cell death. *Biochem Pharmacol* 2016;**116**:1–10.

[34] Häcker H, Tseng PH, Karin M. Expanding TRAF function: TRAF3 as a tri-faced immune regulator. *Nat Rev Immunol* 2011;**11**(7):457–68.

[35] Wang ET, Sandberg R, Luo S, Khrebtukova I, Zhang L, Mayr C, Kingsmore SF, Schroth GP, Burge CB. Alternative isoform regulation in human tissue transcriptomes. *Nature* 2008;**456**(7221):470–6.

[36] Forootan SS, Butler JM, Gardener D, Baird AE, Dodson A, Darby A, Kenny J, Hall N, Cossins AR, Foster CS, Gosden CM. Transcriptome sequencing of human breast cancer reveals aberrant intronic transcription in amplicons and dysregulation of alternative splicing with major therapeutic implications. *Int J Oncol* 2016;**48**(1):130–44.

[37] Shapiro IM, Cheng AW, Flytzanis NC, Balsamo M, Condeelis JS, Oktay MH, Burge CB, Gertler FB. An EMT–driven alternative splicing program occurs in human breast cancer and modulates cellular phenotype. *PLos Genet* 2011;**7**(8):e1002218.

[38] Nooren IM, Thornton JM. Diversity of protein–protein interactions. *EMBO J* 2003;**22**(14):3486–92.

[39] Bishop GA. TRAF3 as a powerful and multitalented regulator of lymphocyte functions. *J Leukocyte Biol* 2016;**100**(5):919–26.

[40] Zhang B, Shetti D, Fan C, Wei K. miR-29b-3p promotes progression of MDA-MB-231 triple-negative breast cancer cells through downregulating TRAF3. *Biol Res* 2019;**52**(1):1–2.

[41] Aronchik I, Bjeldanes LF, Firestone GL. Direct inhibition of elastase activity by indole-3-carbinol triggers a CD40-TRAF regulatory cascade that disrupts NF-κB transcriptional activity in human breast cancer cells. *Cancer Res* 2010;**70**(12):4961–71.